# Crosslinking and Thermal Stability of Thermosets Based on Novolak and Melamine

**Roberto C. Dante,[1] Diego A. Santamaria,[1] Jesús Martín Gil[2]**

[1]*ITT Italia S.r.l., Via S. Martino 87, Barge 12032, CN, Italy*
[2]*Department of Agricultural and Forestry Engineering, University of Valladolid, Campus la Yutera, Avenida de Madrid 44, Palencia 34004, Spain*

Received 22 January 2009; accepted 5 July 2009
DOI 10.1002/app.31114
Published online 19 August 2009 in Wiley InterScience (www.interscience.wiley.com).

**ABSTRACT:** The crosslinking under pressure of a mixture of novolak with melamine resin has been investigated by means of several techniques, including differential scanning calorimetry, thermal gravimetric analysis, X-ray diffraction, and infrared spectroscopy. The crosslinking of the mixture essentially follows two steps. The former occurs at 150°C and leads to resin networks composed of di- and trisubstituted phenols without significant reaction with melamine polymers. The latter, at 200°C, mainly involves the direct crosslinking of melamine polymers with disubstituted phenols. High pressure, applied to the reaction cell, slows down the crosslinking extent, by inhibiting the formation of trisubstituted phenols. This is probably due to the formation of gaseous by-products of crosslinking. Moreover, a certain structuring effect due to high pressure was observed by means of X-ray diffraction.
 J Appl Polym Sci 114: 4059–4065, 2009

**Key words:** crosslinking; curing of polymers; high performance polymers

## INTRODUCTION

Despite the discovering of many classes of materials that act as thermosets, phenolic resins are still widely used in a long list of applications thanks to their low price and commodity of use. There are industrial and commercial interests even a century after Baekeland's invention.[1] Indeed, phenolic resins have a global impact on economy, from the construction sector to the aerospace industry, passing through paper, computers, and many others.[2] The properties of phenolic resins are well exploited and still investigated.[3,4] In fact, phenolic resins are the most common thermosets because of their balance of mechanical properties, such as high hardness,[5] Young's modulus,[6] high thermal stability,[7] creep resistance,[8] and good wetting capability.[9]

The crosslinking process is one of the most crucial aspects of this class of thermosets. Phenolic resin crosslinking is usually carried out through hexamethylenetetramine (HEXA), which forms methylene bridges among the resin polymers. The amount of bridges determines the rigidness and stability of the network, the more the bridges are formed the harder and more stable the crosslinked resin will be. The number of formed bridges will be affected by the application of pressure during the crosslinking, since gaseous by-products are formed. However, high pressures should manifest a certain structuring effect.

In this report, the crosslinking under pressure of a blend of novolak with melamine resin is investigated. Rackley et al.[10] and Santoro et al.[11] found that crosslinking of organic polymers at high pressures raises the number of bonds sufficiently to have an appreciable and permanent effect on density, modulus, and other physical properties. Nevertheless, systems based on novolak cured with HEXA and melamine resin were not deeply investigated till the moment at high pressure. Korošec et al.[12] investigated the curing under pressure of phenolic resin mixed with mold compounds, and found that curing occurs in two successive steps, around 160 and 250°C, respectively. With increasing HEXA content the peak due to the first curing reaction becomes less pronounced at high pressure, whereas the enthalpy of the second increases, indicating a different reaction route.

However, structural XRD studies are mainly focused on the pyrolyzed precursors of either hard or graphitic carbon nitrides,[13] obtained from melamine, and treated under pressure. Melamine resin can be considered as an additional crosslinking agent, and the aforementioned mixture have the potential to achieve a high degree of crosslinking. Crosslinking under pressure was carried out through a special assembled reactor, which works with small amounts of sample (about 300 mg). The crosslinked resins

*Correspondence to:* R. C. Dante (rcdante@yahoo.com).

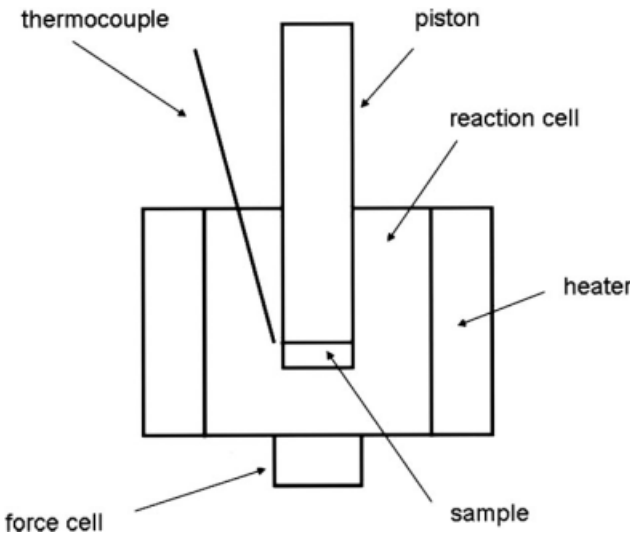


**Figure 1** Sketch of the section of the reactor indicating the main components.

were studied through different experimental techniques, including thermal gravimetric analysis (TGA), differential scanning calorimetry (DSC), X-ray diffraction (XRD), and Fourier transform infrared spectroscopy (FTIR). The main objective of this research report was to understand the effect of both temperature and pressure, on the structure, and the crosslinking mechanism, within the boundaries of the experimental design methodology.

Indeed, the levels of the chosen factors (pressure and temperature) are in the range of those utilized in manufacturing of many phenolic resin based products, such as automotive brake parts. In these field, there is a certain interest into explore the possible new properties introduced by blends of different resins able to crosslink together.

## EXPERIMENTAL SECTION

### Materials

The resins used to study the high pressure crosslinking were novolak resin F4514 produced by Sumitomo Bakelite, Europe, and the melamine resin Hiperesin MF100 C Melamine by Agrolinz Melamine. The resins' mixture was prepared mixing manually the fine powders in a laboratory mortar for about 5 min. The weight percent of melamine resin of the studied binary mixture is 15%.

### Equipments

#### Crosslinking reactor

The resin crosslinking took place inside a small reactor, which was the most crucial element of the experimental setup. The reaction chamber, which hosts the sample, has diameter of 9.3 mm, and is placed upon the force cell. The force cell is placed between the reaction vessel and the PerkinElmer Hydraulic Press. The resin mixture samples were of 300 mg. Figure 1 schematically shows the reactor section (parallel to the direction of load application). During the reaction process, temperature, and load were measured. Temperature was monitored and recorded by means of an ALMEMO sensor 2590-9 V5 series with a portable NiCr-Ni thermocouple and accuracy margin of $\pm 1.5^{\circ}$C. This thermocouple was located close to the sample position (see Fig. 1). The load applied to the reaction cell was measured with a BTT 2000/2 force cell with upper limit of 20,000 N, made by Metior S.r.l., and modified to resist up to 200°C.

#### Chemical and physical characterization techniques of the crosslinked resin mixtures

The characterization of the treated samples was performed by means of several techniques. IR spectroscopy analysis was carried out by means of a FTIR PerkinElmer Spectrum One instrument. Thin tablets of 60 mg, made of the reacted resin specimen and KBr (1 : 25 weight proportion), ground and mixed manually in a laboratory mortar, were prepared under pressure by means of a PerkinElmer Hydraulic Press, at 10 tons. IR spectra were carried out to investigate the changes of absorption due to the crosslinking, in the range of 4000–400 $cm^{-1}$.

The structural evolution of the treated resins was studied by means of XRD with a Philips X'pert spectrometer operating with CuK$\alpha$ radiation. The degradation of the crosslinked materials was investigated by means of the TGA SDTA851 Mettler Toledo with a heating rate of 10°C/min, from 35 to 970°C.

DSC measurements were performed with a heating rate of 10°C/min by the DSC821 Mettler Toledo instrument to measure the crosslinking heat flow, located in the range of 25–250°C.

## RESULTS AND DISCUSSION

### Crosslinking tests

Two levels of both pressure and temperature were considered generating four experiments, named A, B, C, and D, which were carried out by means of the small reactor. The conditions of each experiment are reported in Table I. The temperature curves of the

**TABLE I**
**Experiments' Conditions**

| Experiment | A | B | C | D |
|---|---|---|---|---|
| Maximum T | 150°C | 150°C | 200°C | 200°C |
| Pressure | 140 MPa | 20 MPa | 140 MPa | 20 MPa |
| Duration | 42 min | 42 min | 45 min | 45 min |

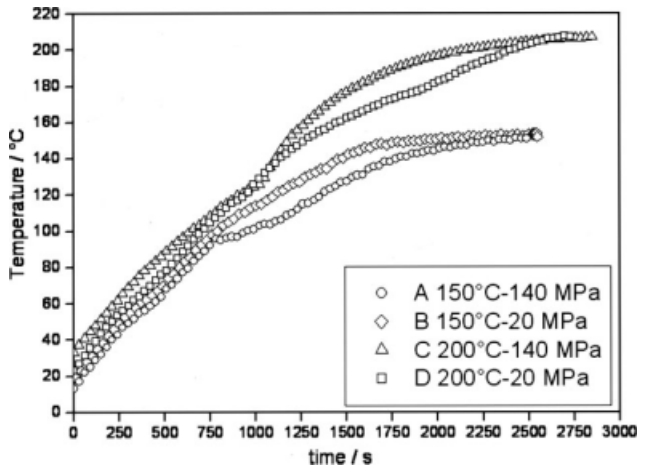


**Figure 2** Temperature curves of the reaction chamber for the four experiments.

reaction chamber for the four experiments are shown in Figure 2. The two temperature levels were: 150 and 200°C, which correspond to the main crosslinking phases found for mixtures of phenolic and melamine resins. The pressure levels were: 20 and 140 MPa, and were chosen spaced enough to provoke different crosslinking, thermal behaviors, and structures. The treatments up to 200°C lasted about 3 min more than those at 150°C, because of the response delay of the heater, especially marked at this temperature level. This brief additional time could have only incremented the reaction extent in the same way for the two experiments, which thus are still comparable. In addition, the temperature of 200°C was chosen to achieve full extent of reaction. Similar experiments were repeated leading to results comparable to those hereinafter reported.

### Differential scanning calorimetry

The DSC curves are shown in Figure 3(a). The DSC curve of the mixture without any previous thermal (called Ref.) exhibits the glass transition at 70°C, while the crosslinking exothermic band is split into two parts: the former peak is sharp around 150°C, only a weak shoulder is present on the left side, whereas the latter is broad, partially overlaps the former and exhibits its maximum around 200°C.

The sample of experiment A shows a significant decrement of the main peak at 150°C, whereas the band at 200°C is clearly shown free of overlapping, indicating that this band is subsequent, and corresponds to a well distinct curing phenomenon. Sample B shows the peak around 150°C further decreased, whereas sample C also shows a considerable reduction of the band around 200°C. However, sample D exhibits only very low residual bands, indicating that the crosslinking reaction was nearly fully completed in the reactor. It is noteworthy to point out that the samples of the experiments A and C, carried out at the higher pressure level (140 MPa), showed residual crosslinking bands (lower extent of reaction) larger than those of the correspondent experiments at lower pressure (20 MPa), B and D, respectively.

The extent of crosslinking after the reactor treatment was calculated for the four experiments through the following equation:

$$\xi = 1 - \frac{H_X}{H_{\mathrm{Ref}}}, \tag{1}$$

where $\xi$ is the extent of crosslinking, $H_{\mathrm{Ref}}$ is the total crosslinking heat per mass unit of the Ref. sample, $H_X$ is the residual heat of the $X$ experiment per mass unit, where $X$ can be A, B, C, or D.

The total heat of crosslinking ($H_{\mathrm{Ref}}$ or $H_X$) equals the area below the DSC crosslinking peaks. The baselines to estimate the area were extrapolated connecting the beginning point of the reaction to the endpoint as shown in Figure 3(a). The so-calculated extents of crosslinking are 58.6, 69.3, 83.5, and 94.2% for experiments A, B, C, and D, respectively. The

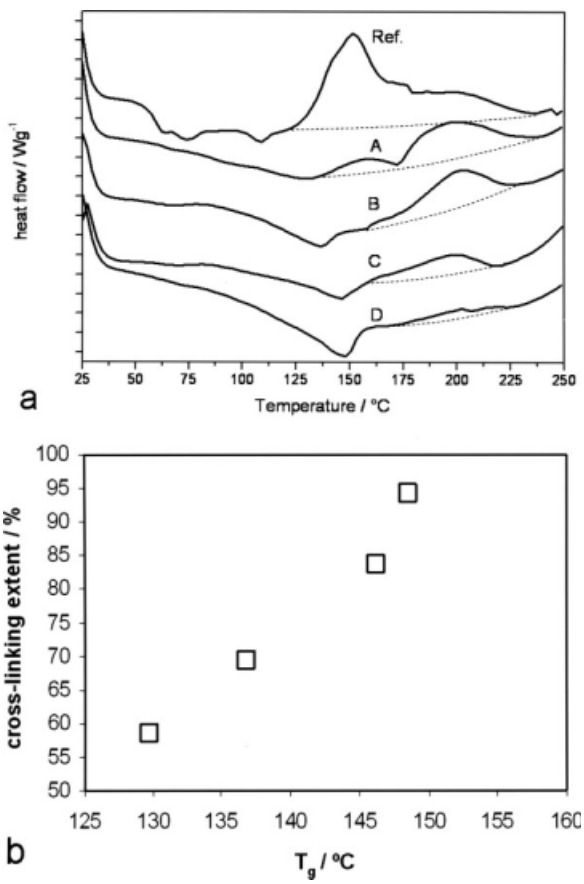


**Figure 3** (a) DSC curves of the treated samples A, B, C, and D. Positive heat flow corresponds to exothermic transformations. The baselines are indicated by dotted lines. (b) Graphic of crosslinking extent as function of $T_g$.

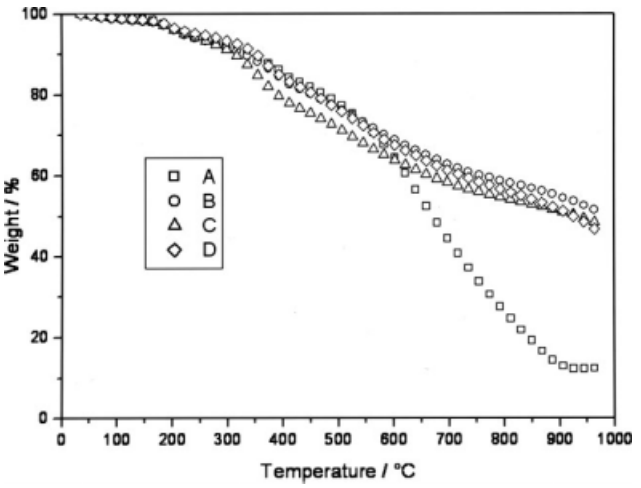


**Figure 4** TGA (under $N_2$) curves of the four treated samples: A, B, C, and D.

DSC results of the four experiments allowed us to distinguish clearly two different crosslinking phases: the first exothermic peak, located at 150°C, and the following exothermic broad band at 200°C reveals.[12] However, high pressure seems to slow down crosslinking extent. Indeed, sample D, treated at the highest temperature level (200°C), and at the lowest pressure level (20 MPa), has the highest reaction extent (94.2%). Figure 3(b) shows the relation between the crosslinking extent and the temperature of the glass transition $T_g$, as found through the DSC curves, and it is possible to observe that advances in crosslinking correspond to shifts of $T_g$ to higher temperatures, as expected, and reported by Gardziella et al.[2]

### Thermal gravimetric analysis

The TGA curves of the four samples, carried out in nitrogen atmosphere, are shown in Figure 4. The behavior of the samples B and D, treated at low pressure (20 MPa), is very similar. The sample of experiment C, obtained at high pressure (140 MPa), but also at high temperature (200°C), has weight loss slightly larger than B and D, starting from 300°C. However, the behavior of sample A is very different from the others, since huge weight loss began from 550°C. Moreover, sample A (see Fig. 4), treated at 150°C and 140 MPa, exhibits the greatest weight loss, reaching up to 90% weight loss at 900°C, in accordance with the lowest calculated reaction extent of 58.6 %, whereas the other samples only lost about the 55%. Nonetheless, other factors, which will be discussed in the "IR spectroscopy" section, characterized the different behavior of sample A. It is noteworthy to point out that, under nitrogen, pyrolysis leads toward the formation of carbonized materials, where prevails the content of carbon and nitrogen with a variable content of hydrogen (about 17% at.), as deeply investigated by Zhao et al.[13] It is noteworthy to point out that FTIR of TGA gaseous by-products (data not reported in the article) shows that samples similar to A exhibit a higher ratio of $HCNO/CO_2$ than the others, indicating that melamine nitrogen is less retained due to the lack of crosslinking with phenolic resin.

### X-ray diffraction

The XRD spectra of the four samples are shown in Figure 5. The spectra were graphically filtered to eliminate only the peaks of aluminum coming from the cell (spikes are present in their positions at 33°, 38°, 45°, and 64°) and those attributable to residual free melamine (spikes at 17°, 24°, 27°, and 29°). The graphical filter was prepared through the Origin program by building a function, which reproduced the impurities' peaks, and was subsequently subtracted to the original spectra. Sample A shows a broad band with maximum at about 18°, and shoulders between 21° and 28°. The amorphous peak around 18° is characteristic of phenolic resins, and is shifted by pyrolysis and thermal treatments to higher angles, toward the 002 reflection of turbostratic carbon structure, which is around 25°.[14–16] Another weaker and broad band is around 42°, which may correspond to a second order of the main amorphous peak, whereas the broad band around 62° may correspond to the third-order reflection of the main amorphous peak. The XRD spectrum of sample B is very similar to that of A, whereas sample C exhibits a shoulder at 20°, apart the maximum at 18.2°, and another shoulder at 28°, in a position similar to that of the reflection of pyrolyzed melamine, which is between 26° and 29°.[13] The spectrum of sample D has the peak maximum shifted to 20°. It should be noticed that the peak

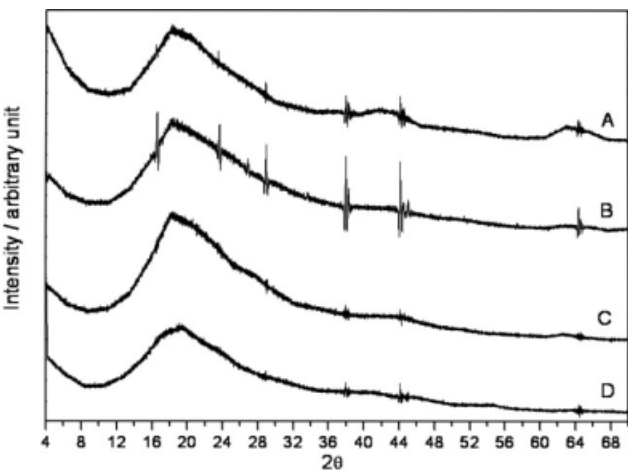


**Figure 5** XRD spectra of the treated samples: A, B, C, and D.

with maximum around 18–20° is always asymmetric for each sample, with a broader right side. The XRD results show that the samples treated at the highest pressure reached higher degree of structuring, although remain amorphous. Indeed, samples A and C, treated at 140 MPa, exhibit bands or shoulders, shifted toward the reflections of turbostratic carbon (002 reflection is around 25°) similar to those of amorphous carbon.

### IR spectroscopy

The whole infrared spectra of the samples after reactor treatment are shown in Figure 6(a), whereas in Figure 6(b), only the region between 1800 $cm^{-1}$ and 400 $cm^{-1}$ is shown to highlight the several significant absorptions of this region. There are several common characteristics of all the spectra. Actually, the spectra show the typical absorptions of phenolic resins. At 3245 $cm^{-1}$, there is the maximum of OH stretching absorption, followed at lower frequencies by the broad absorption due to hydrogen bonds. However, it should be mentioned that, within the OH band, there are other shoulders at higher frequencies (about 3400 $cm^{-1}$) corresponding either to N—H stretching or to other OH types, that is, phenols with different substitution or surroundings from that of the main peak (3245 $cm^{-1}$). The CH stretching of the aromatic ring is positioned at 3000 $cm^{-1}$, whereas $CH_2$ stretching vibrations, which correspond to the bands between 2930 $cm^{-1}$ and 2800 $cm^{-1}$, overlapped the broad OH band. At 1470 $cm^{-1}$, there is a band attributable to $CH_2$ methylene bridge scissor vibrations. At 1330–1326 $cm^{-1}$, there is absorption due to OH bending. CO stretching bands of phenols are positioned between 1240 $cm^{-1}$ and 1060 $cm^{-1}$. Between 1000 $cm^{-1}$ and 1009 $cm^{-1}$, there is the CO stretching absorption of methylol groups (hydrolyzed HEXA or methylols of melamine resin).

The CH out-of-plane deformations of 4-phenol and 2,4-phenol[17] absorb at 820–810 $cm^{-1}$, whereas 2-phenol and 2,6-phenol at 750 $cm^{-1}$,[18] and 2,4,6-phenol at 890–910 $cm^{-1}$.

Around 1600 $cm^{-1}$, there is a doublet due to the aromatic ring C—C stretching vibrations,[19] another peak of the aromatic ring is positioned at 1510 $cm^{-1}$. It is noteworthy to point out that another aromatic ring broad band at about 1550 $cm^{-1}$ is present for samples B, C, and D, probably connected to crosslinking between melamine and phenolic polymers.

The $CH_2$ methylene bridge band at 1470 $cm^{-1}$ of sample A is much lower than that of the other samples, keeping as reference the peak at 1510 $cm^{-1}$. For samples B, C, and D, the bands between 1480 $cm^{-1}$ and 1440 $cm^{-1}$ are more intense than the reference peak at 1510 $cm^{-1}$, indicating an advanced crosslinking. In the case of sample D, the peak at 1470 $cm^{-1}$ is the most intense in the range of 1500 $cm^{-1}$ and 1440 $cm^{-1}$. The relative intensity, $r$, of the band at 1470 $cm^{-1}$, assigned to the $CH_2$ bridges [see Fig. 7(a)] is calculated according to the following equation:

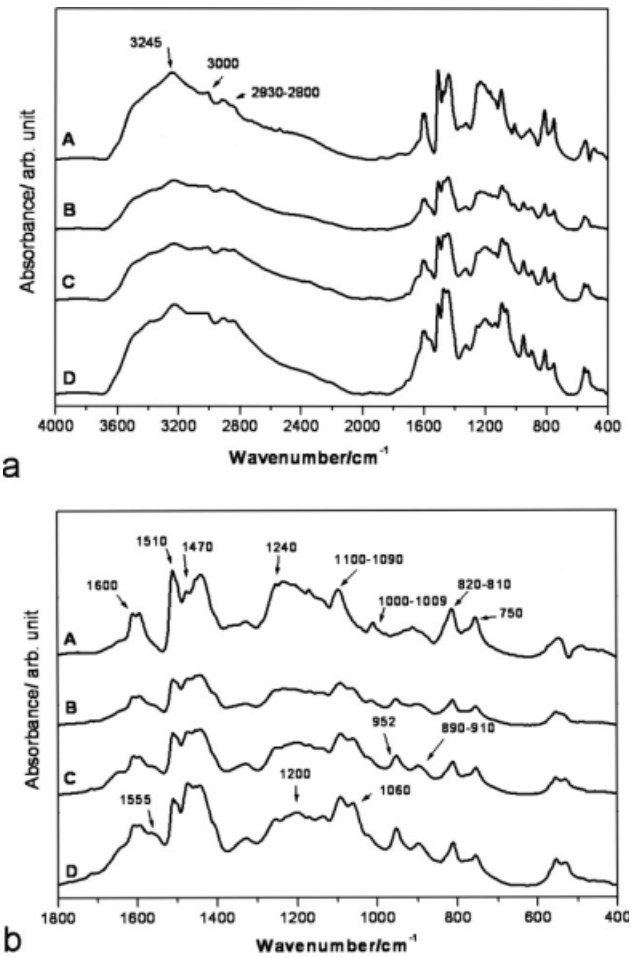


**Figure 6** (a) Whole IR spectra of the treated samples: A, B, C, and D. (b) IR spectra in the region 2000–400 $cm^{-1}$ of the treated samples: A, B, C, and D.

$$r = \frac{\text{absorbance at } 1470\ cm^{-1}}{\text{absorbance at } 1510\ cm^{-1}}. \quad (2)$$

In this equation, the absorbance at 1510 $cm^{-1}$, attributed to the aromatic ring, works as reference, allowing us to compare the IR absorbances of different samples. $r$ is highest for D sample, and lowest for A sample, in accordance with what observed for crosslinking extent (94.2 % for D and 58.6% for A) and TGA. Figure 7(a) points out that pressure decreases the formation of $CH_2$ bridges (crosslinking). In addition, Figure 7(b) shows the correlation between the crosslinking extent and the ratio $r$, which approximately follows the behavior of the

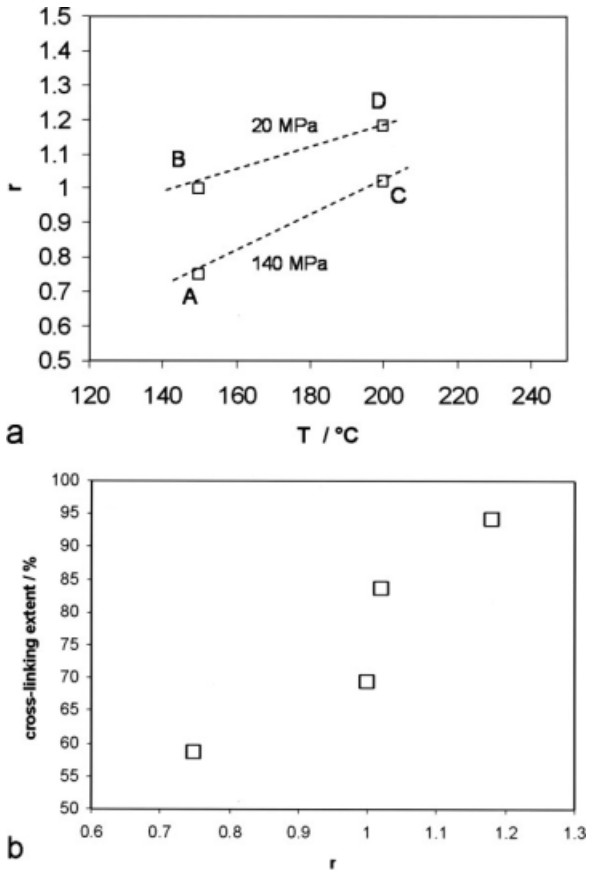


**Figure 7** (a) Graphic of the ratio, named *r*, between the absorbance of the peak at 1470 $cm^{-1}$, and that of the reference peak at 1510 $cm^{-1}$as function of the temperature. (b) Graphic of crosslinking extent as function of the ratio *r*.

graphic of crosslinking extent as function of $T_g$ shift, shown in Figure 3(b).

On the other hand, samples B, C, and D manifest also a band at 952 $cm^{-1}$. The bands between 1100 $cm^{-1}$and 1060 $cm^{-1}$ are more intense than the bands between 1240 $cm^{-1}$ and 1100 $cm^{-1}$. The intensity of the peak at 1090 $cm^{-1}$ seems to be linked to the intensity of the peak at 1470 $cm^{-1}$ related to the methylene bridges, as well as seems to be associated to the band around 890 $cm^{-1}$ and 910 $cm^{-1}$. The peak at 1060 $cm^{-1}$ seems to be associated to the presence of the band at 952 $cm^{-1}$, for example in sample A, both bands are not present. Therefore, the peak at 1090 $cm^{-1}$ can be assigned to the CO stretching of 2,4,6-phenol, as well as the narrow band at 1060 $cm^{-1}$, whereas the bands between 1240 $cm^{-1}$ and 1100 $cm^{-1}$ to the CO stretching of the phenols with lower grade of substitution (probably also with oxygen involved into strong hydrogen bond).

On the basis of the previous arguments, since the band around 890 $cm^{-1}$ and 910 $cm^{-1}$ is attributed to CH out-of-plane deformation of 2,4,6-phenols of the crosslinked phenolic resin, the band at 952 $cm^{-1}$, as the associated band at 1060 $cm^{-1}$, should be attributed to a different type of 2,4,6-phenol, linked to melamine resin through $CH_2$ bridges. Also the aforementioned band at 1555 $cm^{-1}$, more evident in sample D, is connected to the aromatic ring stretching of melamine crosslinked to phenolic resin. Table II resumes the assignments of the main observed bands.

The interpretation of IR spectra clarifies the reaction mechanism to an extent. IR spectrum of sample A (150°C and 140 MPa) show that 2- and 2,4-phenols prevail, involving phenolic resin polymers without significant involvement of melamine polymers, in accordance with DSC and TGA results. Further crosslinking is inhibited by the pressure applied, because gaseous water and ammonia are formed during crosslinking of phenolic polymers by means of HEXA decomposition. The graphics of $T_g$ of Figure 3(b), and that of the ratio *r* of Figure 7(b) are also in accordance with the lower crosslinking degree of sample A, and together with the lack of the highest substituted phenols, can explain the huge weight loss of the TGA curve. The IR spectrum of sample B (150°C and 20 MPa) shows that also that 2,4,6-phenols are present, as well as crosslinking with melamine resin fragments (see new peak at 952 $cm^{-1}$). Since more bridges imply more stability, these facts are in accordance with the higher thermal stability found by TGA of B sample in comparison with A (see Fig. 5). The 952 $cm^{-1}$ peak [Fig. 6(b)] attributed to trisubstituted phenols linked to one

**TABLE II**
**Assignment of Vibrational Modes of IR Spectra of the Reacted Samples**

| Wave number | Vibrational mode |
|---|---|
| 3245 $cm^{-1}$ | OH stretching |
| 3000 $cm^{-1}$ | Aromatic CH stretching |
| 2930–2800 $cm^{-1}$ | $CH_2$ stretching |
| 1600 $cm^{-1}$ and 1510 $cm^{-1}$ | Aromatic C—C stretching |
| 1550 $cm^{-1}$ | Aromatic C—C stretching of phenols crosslinked to melamine resin. |
| 1470–1430 $cm^{-1}$ | $CH_2$ methylene bridge scissor |
| 1240–1060 $cm^{-1}$ | CO stretching bands of phenols |
| 1090 $cm^{-1}$ | CO stretching of 2,4,6-phenol (phenolic resin) |
| 1060 $cm^{-1}$ | CO stretching of 2,4,6-phenol (crosslinking between phenolic resin and melamine resin) |
| 1000–1009 $cm^{-1}$ | CO stretching of methylol groups |
| 952 $cm^{-1}$ | CH out-of-plane deformations of 2,4,6-phenol (crosslinking between phenolic resin and melamine resin) |
| 890–910 $cm^{-1}$ | CH out-of-plane deformations of 2,4,6-phenol (phenolic resin) |
| 820–810 $cm^{-1}$ | CH out-of-plane deformations of 4-phenol and 2,4-phenol |
| 750 $cm^{-1}$ | CH out-of-plane deformations of 2-phenol and 2,6-phenol |

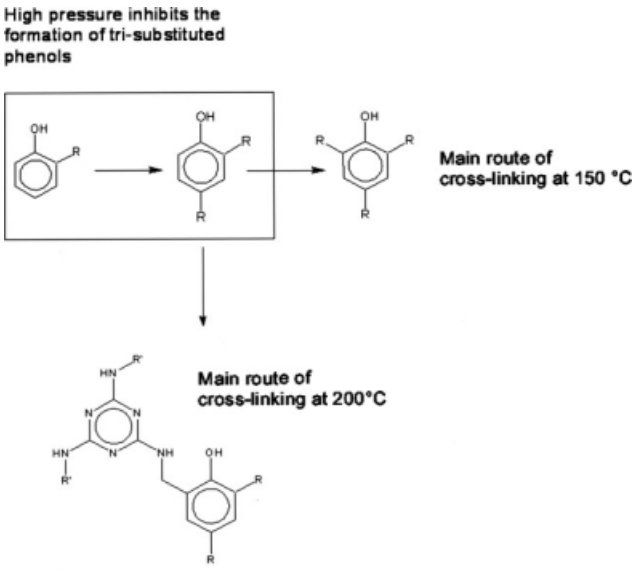


**Figure 8** This sketch depicts how probably the crosslinking mechanism looks like. R stands for phenolic resin polymer, and R′ for melamine resin polymer.

melamine resin fragment is more prominent for the samples treated at 200°C (samples C and D). This indicates that the DSC exothermic band at 200°C can be attributed mainly to the direct crosslinking of phenolic polymers to melamine polymers. Summing up, the scheme of Figure 8 proposes the resin mixture crosslinking mechanism. In the first phase, at 150°C, mainly phenolic resin crosslinking occurs up to have trisubstituted phenols, then, at 200°C, crosslinking is completed by reaction of melamine polymers with disubstituted phenols. However, the application of high pressure (140 MPa) inhibits the extent of the crosslinking, and the creation of an extended network, mainly by inhibiting the formation of trisubstituted phenols and the further reaction with melamine polymers.

It is noteworthy to point out that the crosslinking degree could be incremented by pressure application when solid state reactions are involved,[10,11] which, in any case, would occur at higher pressures than those investigated.

## CONCLUSIONS

The crosslinking of the chosen mixture of phenolic resin and 15% of melamine resin follows two steps: the former at 150°C, where essentially occurs the crosslinking of the phenolic resin, which leads to resin networks composed of di- and trisubstituted ortho (*o*-) and para (*p*-) phenols. The latter at 200°C mainly involves the direct crosslinking of melamine polymers to phenolic polymers to form also trisubstituted phenols, leading to more thermally stable thermosets. The application of high pressure (140 MPa) to the reaction cell reduces the crosslinking extent by inhibiting both the formation of trisubstituted phenols, and the crosslinking between phenolic and melamine polymers, as well as notably decreases the thermal stability of the thermosets. This is probably due to the great amount of gaseous by-products of crosslinking led by HEXA. For example, sample A, treated at 150°C and 140 MPa, exhibits low extent of tri *o, p*-substituted phenols, as well as, no direct reaction with melamine polymers. For instance, only reaching 200°C is possible to have a really crosslinked thermoset of phenolic and melamine resins. However, the samples treated at higher pressure (140 MPa) showed a higher degree of structuring.

The authors are grateful to the DISMIC of Politecnico di Torino for the execution of X-ray diffractions.

## References

1. Baekeland, L. H. Science 1910, 31, 841.
2. Gardziella, A.; Pilato, L. A.; Knop, A. Phenolic Resins: Chemistry, Applications, Standardization, Safety and Ecology; Springer Verlag: Berlin, 2000.
3. Trick, K. A.; Saliba, T. E. Carbon 1995, 33, 1509.
4. Choi, M. H.; Jeon, B. H.; Chung, I. J. Polymer 2000, 41, 3243.
5. Seong, J. K.; Ho, J. Tribol Int 2000, 33, 477.
6. Lee, S. H.; Teramoto, Y.; Shiraishi, N. J Appl Polym Sci 2002, 84, 468.
7. Antony, R.; Pillai, C. K. S. J Appl Polym Sci 2003, 54, 429.
8. Verma, A. P.; Vishwanath, B.; Rao, C. V. S. K. Wear 1996, 193, 193.
9. Bindu, R. L.; Reghunadhan, N. C. P.; Ninan, K. N. Polym Int 2001, 50, 651.
10. Rackley, F. A.; Turner, H. S.; Wall, W. F. Nature 1973, 241, 524.
11. Santoro, M.; Ciabini, L.; Bini, R.; Schettino, V. J Raman Spectrosc 2003, 34, 557.
12. Korošec, R. C.; Mežnar, L. Z.; Bukovec, P. J Therm Anal Calorim 2009, 95, 235.
13. Zhao, Y. C.; Yu, D. L.; Yanagisawa, O.; Matsugi, K.; Tian, Y. J. Diamond Relat Mater 2005, 14, 1700.
14. Ko, T. H.; Chen, P. C. J Mater Sci Lett 2004, 10, 301.
15. Tzeng, S. S.; Chr, Y. G. Mater Chem Phys 2002, 73, 162.
16. Okamura, M.; Takagaki, A.; Toda, M.; Kondo, J. N.; Domen, K.; Tatsumi, T.; Hara, M.; Hayashi, S. Chem Mater 2006, 18, 3039.
17. Liu, C. L.; Ying, Y. G.; Feng, H. L.; Dong, W. S. Polym Degrad Stab 2008, 93, 507.
18. Liu, C. L.; Guo, Q. G.; Shi, J. L.; Liu, L. Mater Chem Phys 2005, 90, 315.
19. Meng, Y.; Dong, G.; Zhang, F.; Shi, Y.; Cheng, L.; Feng, D.; Whu, Z.; Chen, Z.; Wang, Y.; Stein, A.; Zhao, D. Chem Mater 2006, 18, 4447.